



<b>Publication Year</b>	2018
<b>Acceptance in OA</b>	2020-11-09T16:23:12Z
<b>Title</b>	VLT observations of the magnetar CXO J164710.2-455216 and the detection of a candidate infrared counterpart
<b>Authors</b>	TESTA, Vincenzo, MIGNANI, Roberto, Hummel, W., Rea, N., ISRAEL, Gian Luca
<b>Publisher's version (DOI)</b>	10.1093/mnras/stx2574
<b>Handle</b>	<a href="http://hdl.handle.net/20.500.12386/28243">http://hdl.handle.net/20.500.12386/28243</a>
<b>Journal</b>	MONTHLY NOTICES OF THE ROYAL ASTRONOMICAL SOCIETY
<b>Volume</b>	473

# VLT observations of the magnetar CXO J164710.2–455216 and the detection of a candidate infrared counterpart

V. Testa,<sup>1</sup>\* R. P. Mignani,<sup>2,3</sup> W. Hummel,<sup>4</sup> N. Rea<sup>5,6</sup> and G. L. Israel<sup>1</sup>

<sup>1</sup>INAF – Osservatorio Astronomico di Roma, via Frascati 33, I-00078 Monte Porzio Catone, Italy

<sup>2</sup>INAF – Istituto di Astrofisica Spaziale e Fisica Cosmica Milano, via E. Bassini 15, I-20133 Milano, Italy

<sup>3</sup>Janusz Gil Institute of Astronomy, University of Zielona Góra, Lubuska 2, PL-65-265 Zielona Góra, Poland

<sup>4</sup>European Southern Observatory, Karl Schwarzschild-Str. 2, D-85748 Garching, Germany

<sup>5</sup>Institute of Space Sciences (IEEC–CSIC), Carrer de Can Magrans s/n, E-08193 Barcelona, Spain

<sup>6</sup>Anton Pannekoek Institute for Astronomy, University of Amsterdam, Postbus 94249, NL-1090-GE Amsterdam, the Netherlands

Accepted 2017 September 29. Received 2017 September 29; in original form 2017 August 4

## ABSTRACT

We present deep observations of the field of the magnetar CXO J164710.2–455216 in the star cluster Westerlund 1, obtained in the near-infrared with the adaptive optics camera NACO@VLT. We detected a possible candidate counterpart at the *Chandra* position of the magnetar, of magnitudes  $J = 23.5 \pm 0.2$ ,  $H = 21.0 \pm 0.1$  and  $K_S = 20.4 \pm 0.1$ . The  $K_S$ -band measurements available for two epochs (2006 and 2013) do not show significant signs of variability but only a marginal indication that the flux varied (at the  $2\sigma$  level), consistent with the fact that the observations were taken when CXO J164710.2–455216 was in quiescence. At the same time, we also present colour–magnitude and colour–colour diagrams in the  $J$ ,  $H$  and  $K_S$  bands from the 2006 epoch only, the only one with observations in all three bands, showing that the candidate counterpart lies in the main bulk of objects describing a relatively well-defined sequence. Therefore, based on its colours and lack of variability, we cannot yet associate the candidate counterpart to CXO J164710.2–455216. Future near-infrared observations of the field, following up a source outburst, would be crucial to confirm the association with the detection of near-infrared variability and colour evolution.

**Key words:** stars: neutron – pulsars: individual: CXOJ164710.2-455216.

## 1 INTRODUCTION

The *Chandra* X-ray source CXO J164710.2–455216 was discovered in the massive star cluster Westerlund 1 (Muno et al. 2006) as a bright X-ray source, modulated at a period of 10.6 s identified as the spin period  $P_s$  of an isolated neutron star (INS), as suggested by the lack of a bright infrared (IR) counterpart. The period value is typical of that of a peculiar class of INSs, the magnetars, of which about 30 are known to date, as listed in the McGill Magnetar Catalogue (Olausen & Kaspi 2014).<sup>1</sup> Magnetars are thought to be INSs with enormous magnetic fields in excess of  $10^{14}$  G, hence the name, which are powered by magnetic energy instead of the star rotation (see Kaspi & Beloborodov 2017 for a recent review). The blackbody (BB) X-ray spectrum ( $kT = 0.61$  keV) of CXO J164710.2–455216, the size of the emitting radius ( $r_{\text{BB}} \sim 0.3$  km), the X-ray luminosity ( $L_X \sim 3 \times 10^{33}$  erg s<sup>-1</sup>), in excess of the pulsar rotational energy loss  $\dot{E} \sim 3 \times 10^{31}$  erg s<sup>-1</sup>, as inferred from the period derivative

$\dot{P}_s$  (Israel et al. 2007; Rodriguez Castillo et al. 2014), the inferred dipolar magnetic field of  $\sim 10^{14}$  G, are also typical of magnetars. The detection of a bright X-ray outburst (Krimm et al. 2006) is also in line with the classical magnetar behaviour. The outburst decay has been followed through the years with all X-ray observing facilities (Israel et al. 2007; Naik et al. 2008; Woods et al. 2011; An et al. 2013) and is consistent with trends observed in other magnetars. The association of CXO J164710.2–455216 with Westerlund 1 has suggested that the magnetar progenitor was an extremely massive star of mass  $\gtrsim 50 M_\odot$  (Muno et al. 2006; Belczynski & Taam 2008), more massive than expected according to INS formation theories that predict progenitors of mass  $\approx 10 M_\odot$ . It has also been suggested that CXO J164710.2–455216 possibly formed in a binary system, now disrupted after the progenitor star went supernova, with the star Wd1-5 being the pre-supernova companion (Clark et al. 2014).

Very little is known about the optical and IR emission properties of magnetars and the underlying emission mechanisms (e.g. Mereghetti 2011; Mignani 2011). Indeed, magnetars are elusive targets in the optical/IR, owing to their usually large distances and interstellar extinction, and only nine of them have been

\* E-mail: vincenzo.testa@oa-roma.inaf.it

<sup>1</sup> <http://www.physics.mcgill.ca/~pulsar/magnetar/main.html>

identified in the optical and/or near-IR out of the 30 currently known (Olausen & Kaspi 2014) with a flux measurement in at least one filter. Their magnetar IR emission is probably non-thermal in origin with an higher emission efficiency with respect to rotation-powered pulsars, possibly related to their much higher magnetic fields (Mignani et al. 2007). Emission from a debris disc might explain the magnetar emission in the mid-IR (Wang, Chakrabarty & Kaplan 2006a). No optical/IR counterpart has been detected for CXO J164710.2–455216 from observations carried out soon after the magnetar discovery (Muno et al. 2006; Wang et al. 2006b). No other IR observations of this magnetar have been reported ever since.

Here, we present the results of near-IR observations of the magnetar carried out in two different epochs with the Very Large Telescope (VLT). This manuscript is structured as follows: observations and data analysis are presented in Section 2, whereas the results are presented in Sections 3 and 4, respectively.

## 2 OBSERVATIONS, REDUCTIONS AND CALIBRATIONS

The data set consists of two epoch observations of the field of CXO J164710.2–455216 obtained with the VLT@ the ESO–Paranal Observatory (Chile), equipped with the NAOS–CONICA Adaptive Optics (AO) camera (NACO; Lenzen et al. 2003; Rousset et al. 2003). In both epochs, the NACO S27 camera was used, with a field of view of  $27 \text{ arcsec} \times 27 \text{ arcsec}$  and a scale of  $0.027 \text{ arcsec pixel}^{-1}$ . We retrieved the first epoch data from the public ESO archive,<sup>2</sup> while the second epoch data were obtained via a dedicated proposal submitted by our group (Programme ID: 091.D-0071(B), PI Mignani). For the first epoch – 2006 June 26 and 27, images were taken in the three wide bandpass  $J$ ,  $H$ ,  $K_S$  filters, while in the second epoch – 2013 August 16, only the  $K_S$  filter was used. Images were taken using the double-correlated read-out mode with several single dithered frames (DIT) repeated  $n$ -times (NDIT) and stacked together along each node of the dithering pattern. The choice of DIT and NDIT depends on the used filter and the epoch. In particular, DIT is usually shorter in the long wavelength filters because of the higher background level. For the first epoch data set a total of 2520, 2070 and 1870 s of integration time was obtained for the  $J$ ,  $H$  and  $K_S$  filters, respectively, while for the second epoch one a total of 7425 s of integration time in the  $K_S$  was secured. For each epoch, and each filter, single images were pre-reduced (flat fielding, sky subtraction, exposure map correction) and co-added through the NACO pipeline obtaining a master image. The full width half-maximum (FWHM) of a point source computed on each master image is 0.123 arcsec, 0.106 arcsec and 0.110 arcsec for the  $J$ ,  $H$  and  $K_S$  filters of the first epoch, and 0.116 arcsec for the  $K_S$  of the second epoch.

Object photometry was performed by means of the widely-used package DAOPHOT II (Stetson 1994) which we used to obtain multi-band catalogues of all objects found in the NACO images down to a detection limit of  $\sim 5\sigma$  over the background. We calibrated our object catalogues via comparison with the 2MASS Point Source Catalogue (Skrutskie et al. 2006), which was also used to compute the astrometric solution for the NACO images. This last process presented some difficulties because it may happen that a single 2MASS star is actually resolved in a multiple object on the almost diffraction-limited NACO images, so that the astrometric calibration has to be performed carefully to prevent systematics. More-

over, in a field of view as small as that of NACO, only very few 2MASS stars are present, and generally affected by strong saturation and/or non-linearity problems. In order to bypass this problem, we computed the astrometric calibration via a two-step process using an archival  $K$ -band image of the field taken with the Son Of Isaac (SOFI) infrared Camera at the ESO New Technology Telescope (NTT). As a first step, we calibrated the astrometry of the SOFI image, of area  $\approx 4 \text{ arcmin} \times 4 \text{ arcmin}$ , by using the 2MASS and UCAC4 (Zacharias et al. 2013) catalogues. Then, we used a catalogue of secondary stars detected on the SOFI image, fainter than the 2MASS stars and with many more matches on the NACO images, to derive their final astrometric solution. In this way, we obtained an astrometric solution with an overall uncertainty of about 87 mas, coming from the error propagation on the differences in position in the sense (found-reference) to which the high-end of the overall precision figure of the 2MASS survey ( $80 \text{ mas}^3$ ) has been added in quadrature. Analogously, photometric calibration via 2MASS shows the same potential problem, and in case a 2MASS star is resolved in a multiple object, a correct calibration is obtained by summing up the fluxes of all the stars which appear as a single blended object in the 2MASS catalogue. In order to circumvent this problem, and also considering that the bright 2MASS stars are in general non-linear in the NACO images, we adopted the two-step calibration via SOFI images also for the photometric calibration. At the end of the process, the obtained zero-points have an uncertainty of  $\sim 0.1 \text{ mag}$  in all three filters and two epochs.

Since we are interested in detecting a possible variability of the candidate counterpart(s) to CXO J164710.2–455216, which is traditionally considered as a marker of the identification of a magnetar counterpart, e.g. Tam et al. (2004), particular attention has been devoted to relative calibration of one dataset against the other in the only filter for which we had two-epochs data, the  $K_S$  one. In this way, glitches and systematics possibly affecting the absolute photometric calibration process are strongly reduced. We remind, however, that the lack of IR variability, correlated or not with variations in the X-ray flux (see e.g. Durant & van Kerkwijk 2006), does not necessarily argue against a potential counterpart identification. For instance, in the case of the IR counterpart to the magnetar XTE J1810–197 variations of the IR flux do not follow the same trend observed in the X-ray (Testa et al. 2008).

## 3 NEAR-IR CANDIDATE COUNTERPART

Fig. 1 shows an  $\sim 3 \text{ arcsec} \times 3 \text{ arcsec}$  map of an area centred on the nominal coordinates of CXO J164710.2–455216. The different depth due to the much longer exposure time of the second epoch image can be appreciated by eye. In both maps, circles are drawn at the nominal CXO J164710.2–455216 position, with radius corresponding to the 90 percent positional uncertainty of the X-ray source. This has been calculated by adding in quadrature the uncertainty on the primary astrometric calibrators (2MASS,  $80 \text{ mas}$  – we adopt the higher end of the range given in the catalogue), the internal r.m.s. of the astrometric fit, which is considerably smaller ( $0.4 \text{ pixels} = 0.011 \text{ arcsec}$  or  $11 \text{ mas}$ ), and the uncertainty of the CXO J164710.2–455216 position. We computed the coordinates of CXO J164710.2–455216 from the available *Chandra* observations of the field. In particular, we used three ACIS-S observations (Obs Id.: 5411, 6283, 14360) taken in the imaging mode where the pulsar has always been observed on the axis and located on

<sup>2</sup> www.eso.org/archive

<sup>3</sup> www.ipac.caltech.edu/2mass/releases/allsky/doc/sec2\_2.html

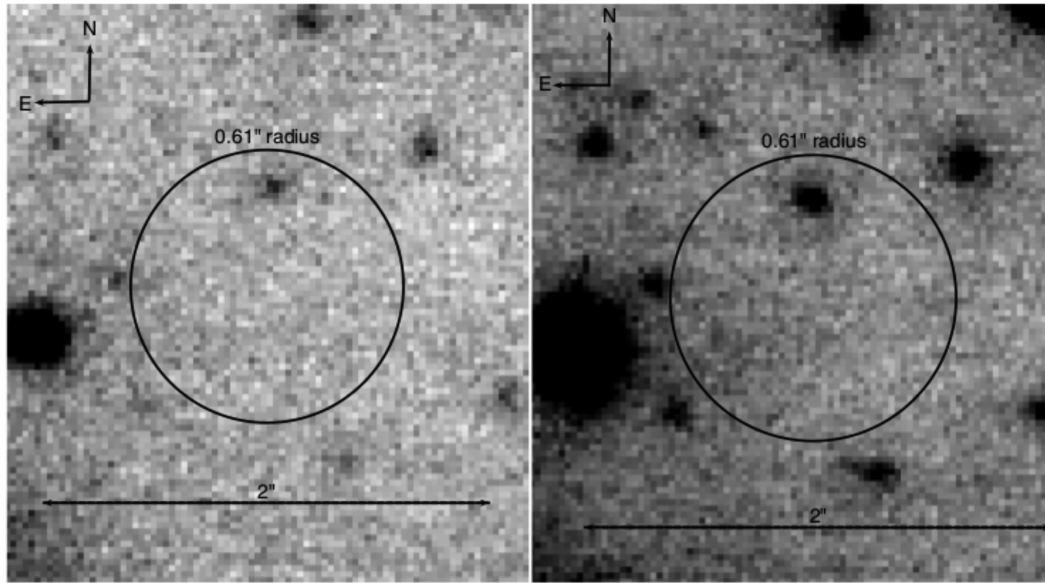


**Figure 1.** Zoom of the CXO J164710.2–455216 field around its *Chandra* position taken in the  $K_S$ -band at two different epochs. Left: 2006 June, right: 2013 August. The circle is drawn at the *Chandra* position of CXO J164710.2–455216 and has a radius equal to the overall 90 per cent confidence level position uncertainty (0.61 arcsec).

the back-illuminated chip S3, which is optimized for source positioning. We derived average coordinates of  $\alpha = 16^{\text{h}}47^{\text{m}}10^{\text{s}}.21$ ;  $\delta = -45^{\circ}52'17''.06$ , where the statistical error on the position is negligible with respect to the systematic uncertainty on the absolute *Chandra* astrometry, which is 0.6 arcsec at the 90 per cent confidence level.<sup>4</sup> An attempt was made to improve the accuracy of the *Chandra* astrometry and to reduce the uncertainty on the position of our target by using other sources detected in the ACIS-S chip 3 field of view. We found several X-ray sources in the *Chandra* images of CXO J164710.2–455216. However, the aim point of these images is the core of the Westerlund 1 cluster, where the high density of objects makes it extremely difficult to associate an X-ray source with a high-confidence candidate counterpart, even at the *Chandra* spatial resolution. Indeed, all our attempts resulted in a large scatter around the best-fitting match between the X-ray coordinates and the optical/IR ones, comparable to (or larger than) the nominal 90 per cent *Chandra* absolute astrometry accuracy. Therefore, a conservative approach was adopted and the above value was used. We note that the overall uncertainty of our astrometry is much larger than any reasonable figure of the positional uncertainty due to an unknown proper motion of the source. For instance, assuming an average neutron star velocity of  $400 \text{ km s}^{-1}$  (Hobbs et al. 2005) and a distance of 5 kpc would give a figure of  $0.016 \text{ arcsec yr}^{-1}$ .

As can be seen from the map(s) in Fig. 1, one object clearly falls within the error circle. There are other faint fluctuations visible within the error circle, but those have marginal significance, around or below  $1\sigma$  and are undetected by the source detection algorithm of DAOPHOT, even when pushed to very faint detection limits, and we regard them as background fluctuations, although they might deserve further attention should any deeper observation ever be carried out in the future. As far as our results show, we assume the object in the error circle as the candidate IR counterpart of CXO J164710.2–455216. Its magnitudes are  $K_S = 20.4 \pm 0.1$  and  $K_S = 20.0 \pm 0.1$  in the 2013 and 2006 images, respectively. For

the  $J$  and  $H$  filters, available as we said for the first epoch only, we find:  $J = 23.5 \pm 0.2$  and  $H = 21.0 \pm 0.1$ . No other object has been detected down to  $3\sigma$  magnitude limits of 23.6, 22.3, 21.1 in  $J$ ,  $H$ ,  $K_S$ , respectively (first epoch), whereas the  $K_S$ -band limit for the second epoch is deeper, namely  $K_S = 21.9$ .

Given the large number of stars in the crowded Westerlund 1 field the chance coincidence probability to find an object within a radius of 0.61 arcsec is quite high. The probability  $P = 1 - \exp(-\pi\rho r^2) \sim 90$  per cent, where  $r = 0.61$  arcsec and  $\rho \sim 2 \text{ arcsec}^{-2}$  is the number density of objects in the NACO field of view measured in the  $K_S$ -band image. However, we cannot rule out a priori that this object is, indeed, associated with CXO J164710.2–455216.

Our candidate might be one of the ‘two very faint objects’ found near the X-ray source position in observations obtained on 2006 May 17 with PANIC (Persson’s Auxilliary Nasmyth Infrared Camera) at the 6.5 m Magellan-Baade telescope (Las Campanas) by Wang et al. (2006b), when the source was in quiescence. These ‘two very faint objects’ were not detected in PANIC follow-up observations of the CXO J164710.2–455216 X-ray outburst (Krimm et al. 2006) taken on 2006 September 29 (Wang et al. 2006b). This suggested that neither of them could have been the magnetar counterpart, for which a brightening of  $\sim 4.6$  mag would have been expected if the IR flux of the magnetar scales exactly as the X-ray flux (e.g. Tam et al. 2004). In this case, the ratio between the observed X-ray flux in outburst and in quiescence (Muno et al. 2006) would translate into the expected variation of 4.6 mag in the IR flux (Wang et al. 2006b). However, Wang et al. (2006b) did provide a finding chart nor a reference magnitude, so that we cannot tell if our candidate counterpart is one of their ‘two very faint objects’ and any comparison with their results would be, at this point, just speculative. Our limits are slightly fainter than those obtained by Wang et al. (2006b,  $K_S \sim 21$ ) for the 2006 data and one magnitude fainter for the 2013 ones. Fig. 2 shows the colour–magnitude (CMD) and colour–colour (CCD) diagrams of the catalogue of objects in common between the two epochs. The position of the CXO J164710.2–455216 candidate counterpart is highlighted with

<sup>4</sup> <http://xc.harvard.edu/ciao/ahelp/coords.html>

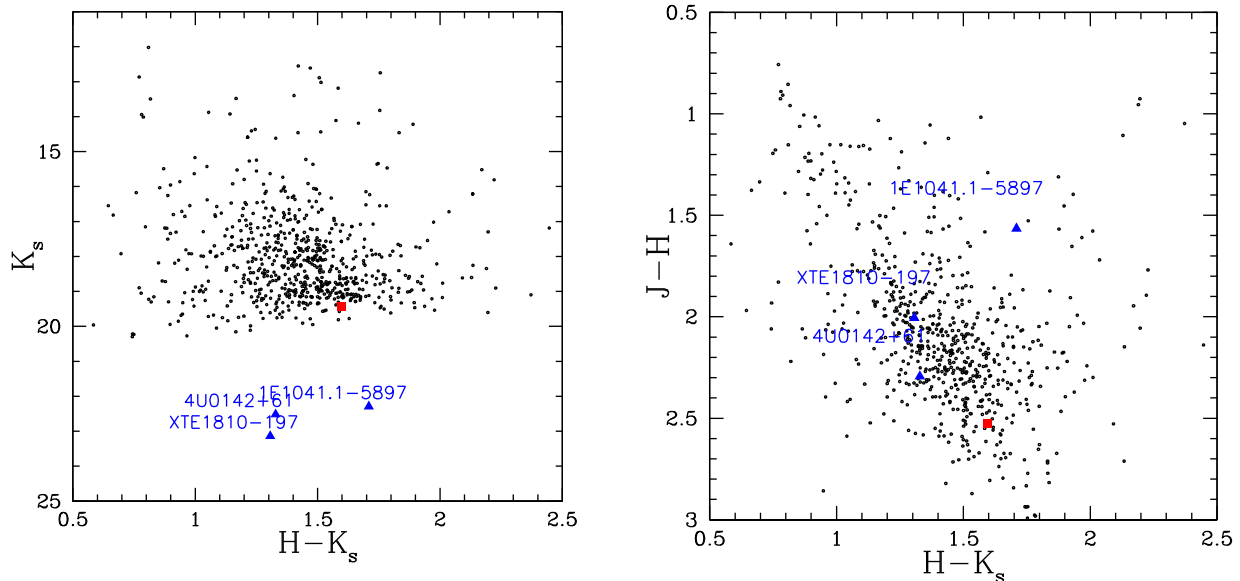


**Figure 2.** CMD (left) and CCD (right) for all sources in the CXO J164710.2–455216 NACO field of view. The candidate counterpart is marked with a red square dot. The blue triangles correspond to magnetars with magnitudes in all the three near-IR filters, plotted as a reference. Their observed fluxes have been scaled according to the nominal reddening and distance values. All values are from the Mc Gill Magnetar Catalogue and references therein.

a larger, red square dot. The candidate has magnitudes and colours of the bulk of stars redder than the main sequence which might belong to the field population (see Kudryavtseva et al. 2012 for an analysis of the cluster population), despite what would be expected if it was the actual counterpart of CXO J164710.2–455216. For comparison, Fig. 2 also shows the observed colours for a sample of magnetars with detections in the  $J$ ,  $H$  and  $K_S$  bands, where the flux values have been taken from the Mc Gill Magnetar catalogue. As seen, at variance with the CXO J164710.2–455216 candidate counterpart, the colours of the magnetar counterparts are quite bluer from those of a field stellar population, not to mention the fact that the magnitudes of known magnetars, scaled to the distance and reddening of Westerlund 1 are fainter than our candidate. However, very little is still known on the magnetars’ near-IR spectra and on their evolution with the source state, which means that assuming magnetar colours derived from flux measurements that might have been obtained at different epochs as a template has to be done with due caution. Indeed, our first epoch NACO observations were taken within 1 d from each other and when the source was in quiescence (see below). Moreover, magnetars’ luminosities in the near-IR can differ by three orders of magnitude (e.g. Mignani et al. 2007), so that none of them can be assumed as a ‘standard candle’.

It is interesting to note that both NACO observations were carried out while the source was in quiescence, since the first epoch (2006 June) falls before the outburst detected in 2006 September (Krimm et al. 2006), and the second epoch one (2013 August) falls after another less intense burst which has been registered in 2011 November. No other outbursts have been registered ever since (see Rodriguez Castillo et al. 2014, and references therein for details), till the very recent one occurred on 2017 May 16 (D’Ai et al. 2017). Fig. 3 shows a comparison plot of the 2013 versus 2006  $K_S$ -band magnitudes for a number of objects in a restricted area around the position of CXO J164710.2–455216, aimed at studying the variability of its candidate counterpart. The plot shows signs of variation of the candidate counterpart, but they are well within the uncertainties at about a  $2\sigma$  level, consistent with the hypothesis that the source did not vary its IR flux from the first to the second of

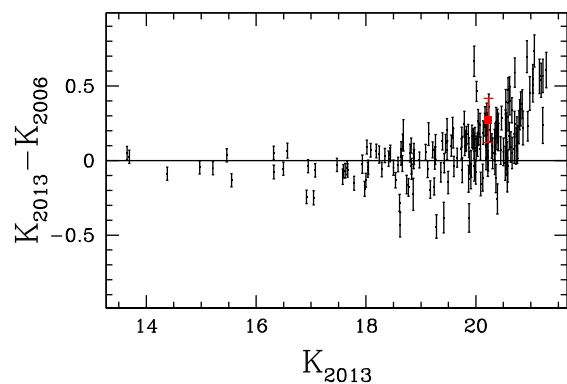


**Figure 3.** Difference between the  $K_S$ -band magnitudes of the CXO J164710.2–455216 candidate counterpart as measured in the first (2006 June) and second (2013 August) epochs of the NACO observations. The red point corresponds to the candidate counterpart, whereas the black dots correspond to field stars selected in the object vicinity within 300 pixels and with good photometry.

the two epochs. This is not surprising if one takes into account the quiescence of the magnetar at both epochs. If the object that we detected in the *Chandra* error circle of CXO J164710.2–455216 was its actual counterpart, it would have a  $K_S$ -band luminosity of  $\sim 1.12 \times 10^{31} \text{ erg s}^{-1}$ , at the Westerlund 1 distance of 5 kpc and assuming the  $K_S$ -band interstellar extinction from the Mc Gill Magnetars’ catalogue ( $A_K = 1.4$ ). This luminosity would be about 37 per cent of the pulsar rotational energy loss, a quite high fraction but still comparable to those of other magnetars and in line with the CXO J164710.2–455216 magnetic field of  $10^{14} \text{ G}$  (Mignani et al. 2007). The observed  $K_S$ -band-to-X-ray flux ratio would be  $\sim 6.1 \times 10^{-3}$ , where the X-ray flux in quiescence has been measured in the 1–10 keV energy band, still in the range typical of magnetars (Rea et al. 2010). Therefore, at least according to its expected near-IR luminosity and near-IR/X-ray emission, the source that we detected in the CXO J164710.2–455216 error circle would still be a plausible candidate counterpart.

#### 4 SUMMARY AND CONCLUSIONS

In this study, we present an attempt to identify the near-IR counterpart to the magnetar CXO J164710.2–455216 by means of AO observations obtained in two epochs, the first one before the outburst of 2006 (Krimm et al. 2006) and the second one well after the second outburst in 2011. We identify a main candidate within the 90 percent confidence level error circle around the nominal position of CXO J164710.2–455216. About the candidate, it shows no obvious variability between the two epochs, but this is an expected result since the X-ray source was in a quiescent state at both epochs. Moreover, the candidate has the characteristics of a main-sequence star showing no particular colours, which would be expected for a magnetar. Monitoring the evolution of the source brightness in the near-IR, following outburst activities in the X-ray, would be crucial to determine whether this source is the actual counterpart to CXO J164710.2–455216. Nevertheless, new deeper observations with AO-equipped large telescopes, e.g. the forthcoming ELTs, are needed to confirm if the candidate is really the magnetar counterpart and, in case of success, determine its nature.

#### ACKNOWLEDGEMENTS

This paper is based on observations collected at the European Organization for Astronomical Research in the Southern hemisphere under ESO programme 091.D-0071(B). We thank the anonymous referee for his/her considerate and constructive review of our manuscript. RPM acknowledges financial support from an ‘Occhialini Fellowship’.

#### REFERENCES

An H., Kaspi V. M., Archibald R., Cumming A., 2013, *ApJ*, 763, 82  
 Belczynski K., Taam R. E., 2008, *ApJ*, 685, 400  
 Clark J. S., Ritchie B. W., Najjarro F., Langer N., Negueruela I., 2014, *A&A*, 565, 90

D’Ai A., Evans P. A., Krimm H. A., Kuin N. P. M., Lien A. Y., Page K. L., 2017, *GCN Circulars No.* 21095  
 Durant M., van Kerkwijk M., 2006, *ApJ*, 652, 576  
 Hobbs G., Lorimer D. R., Lyne A. G., Kramer M., 2005, *MNRAS*, 360, 974  
 Israel G. L., Campana S., Dall’Osso S., Muno M. P., Cummings J., Perna R., Stella L., 2007, *ApJ*, 664, 448  
 Kaspi V. M., Beloborodov A., 2017, *ARA&A*, 55, 261  
 Krimm H., Barthelmy S., Campana S., Cummings J., Israel G., Palmer D., Parsons A., 2006, *GCN Circulars No.* 5581  
 Kudryavtseva N. et al., 2012, *ApJ*, 750, L44  
 Lenzen R. et al., 2003, *Proc. SPIE*, 4841, 944  
 Mereghetti S., 2011, *Adv. Space Res.*, 47, 1317  
 Mignani R. P., 2011, *Adv. Space Res.*, 47, 1281  
 Mignani R. P., Perna R., Rea N., Israel G. L., Mereghetti S., Lo Curto G., 2007, *A&A*, 471, 265  
 Muno M. P. et al., 2006, *ApJ*, 636, L41  
 Naik S. et al., 2008, *PASJ*, 60, 237  
 Olausen S. A., Kaspi V. M., 2014, *ApJS*, 212, 60  
 Rea N. et al., 2010, *MNRAS*, 407, 1887  
 Rodriguez Castillo G. A. et al., 2014, *MNRAS*, 441, 1305  
 Rousset G. et al., 2003, *Proc. SPIE*, 4839, 140  
 Skrutskie M. F. et al., 2006, *AJ*, 131, 1163  
 Stetson P. B., 1994, *PASP*, 106, 250  
 Tam C. R., Kaspi V. M., van Kerkwijk M. H., Durant M., 2004, *ApJ*, 617, L53  
 Testa V. et al., 2008, *A&A*, 482, 607  
 Wang Z., Chakrabarty D., Kaplan D. L., 2006a, *Nature*, 440, 772  
 Wang Z., Kaspi V. M., Osip D., Morrel N., Kaplan D. L., Chakrabarty D., 2006b, *Astron. Telegram*, 910  
 Woods P. M., Kaspi M., Vi. Gavriil F. P., Airhart C., 2011, *ApJ*, 726, 37  
 Zacharias N., Finch C. T., Girard T. M., Henden A., Bartlett J. L., Monet D. G., Zacharias M. I., 2013, *AJ*, 145, 44

This paper has been typeset from a  $\text{\TeX}/\text{\LaTeX}$  file prepared by the author.